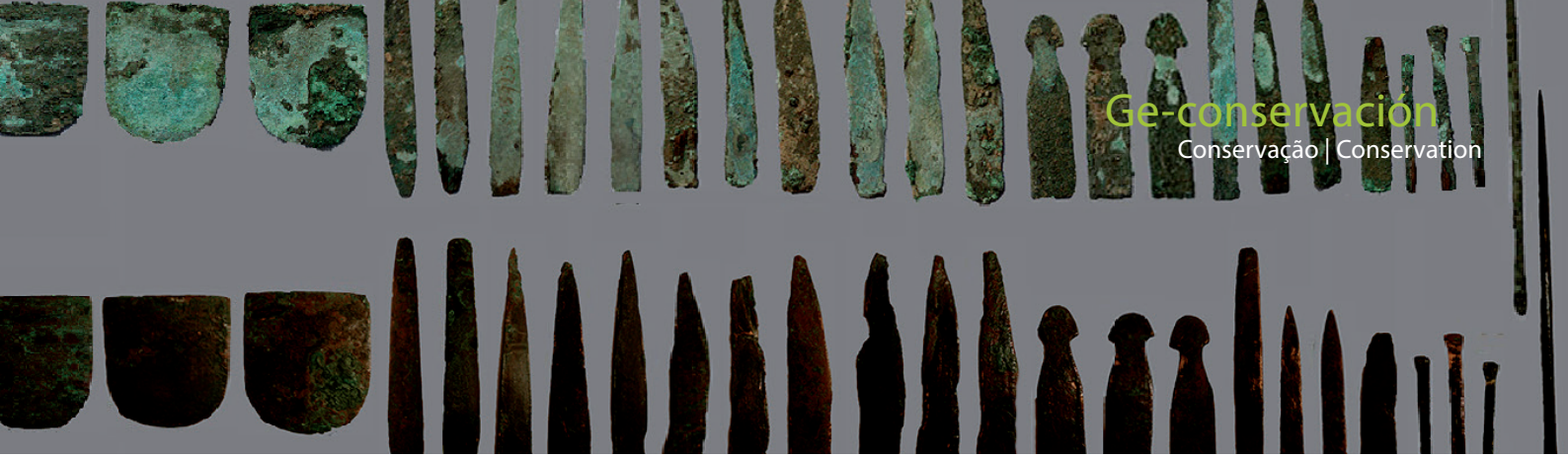

Multianalytical Investigation and Conservation of Unique Copper Model Tools from Ancient Egyptian Dark Age

Manal Maher, Yussri Salem

Abstract: The article presented multianalytical investigation of a unique set of copper model tools dated back to Dark Age, from the tomb of KHENNU AND APA-EM-SA-F (289) in the south of Memphis, Saqqara. Stereomicroscope was used to examine the morphology of outer surface corrosion products. Metallographic microscope was used to investigate the microstructure of the metal core and the stratigraphy of corrosion layers. SEM-EDX was used to identify the elemental composition of the objects. XRD and Raman spectroscopy were used to analyze the outer surface and the internal corrosion respectively. The microscopic investigation revealed the corrosion layers consists of external layer, under-surface layer and internal corrosion products. Cuprite, paratacamite, nantokite, atacamite, malachite and chalconatronite were identified by XRD and Raman spectroscopy as a surface and internal corrosion. SEM-EDX revealed that the case-study objects consist of copper metal without any further alloying elements. The study presented suitable treatment for these friable objects or such cases, and then presented a safe fixing procedure by a sewing technique via transparent inert threads.

Keyword: Dark Age, copper model tools, first intermediate period, corrosion products, transparent inert threads

Investigación multianalítica y conservación de herramientas de cobre únicas de la Edad oscura del Antiguo Egipto

Resumen: El artículo presentó una investigación multianalítica de un conjunto único de herramientas de cobre que se remonta a la Edad Oscura, de la tumba de KHENNU Y APA-EM-SA-F (289) en el sur de Memphis, Saqqara. Se utilizó estereomicroscopio para examinar la morfología de los productos de corrosión de la superficie exterior. Se utilizó un microscopio metalográfico para investigar la microestructura del núcleo metálico y la estratigrafía de las capas de corrosión. Se utilizó SEM-EDX para identificar la composición elemental de los objetos. Se utilizó espectroscopía XRD y Raman para analizar la superficie externa y la corrosión interna, respectivamente. La investigación microscópica reveló que las capas de corrosión consisten en una capa externa, una capa debajo de la superficie y productos de corrosión internos. Cuprita, paratacamita, nantokita, atacamita, malaquita y calconatronita fueron identificadas por espectroscopía XRD y Raman como corrosión superficial e interna. SEM-EDX reveló que los objetos del estudio de caso consisten en metal de cobre sin ningún elemento de aleación adicional. El estudio presentó un tratamiento adecuado para estos objetos friables o tales casos, y luego presentó un procedimiento de fijación seguro mediante una técnica de costura a través de hilos inertes transparentes.

Palabras clave: Edad Oscura, herramientas de modelo de cobre, primer período intermedio, productos de corrosión, hilos inertes transparentes

Investigação multianalítica e conservação de ferramentas de cobre únicas da Idade Média do Antigo Egito

Resumo: O artigo apresenta uma investigação multianalítica de um conjunto único de ferramentas modelo de cobre datadas da Idade Média, da tumba de KHENNU E APA-EM-SA-F (289) no sul de Memphis, Saqqara. Foi usado um estereomicroscópio para examinar a morfologia dos produtos de corrosão da superfície externa. Foi utilizado um microscópio metalográfico para investigar a microestrutura do núcleo metálico e a estratigrafia das camadas de corrosão. Utilizou-se a espectroscopia SEM-EDX para identificar a composição elementar dos objetos. A espectroscopia XRD e de Raman foram usadas para analisar a superfície externa e a corrosão interna, respetivamente. A investigação microscópica revelou que as camadas de corrosão consistem numa camada externa, numa camada abaixo da superfície e em produtos de corrosão internos. Foram identificados cuprite, paratacamite, nantoquite, atacamite, malaquite e calconatronite por XRD e por espectroscopia Raman como corrosão superficial e interna. SEM-EDX revelou que os objetos do estudo

de caso consistem em metal de cobre sem quaisquer outros elementos de liga. O estudo apresentou um tratamento adequado para esses objetos friáveis ou casos similares, e apresentou um procedimento de fixação seguro mediante uma técnica de costura e através de fios inertes transparentes.

Palavras-chave: Idade Média, ferramentas modelo de cobre, primeiro período intermediário, produtos de corrosão, fios inertes transparentes

Introduction

Dark Age is a term described the first intermediate period in the ancient Egyptian history (c.2181–2055 BC). This era was succeeded the old kingdom (c.2613-2181 BC) and preceded the middle kingdom (2040-1782 BC). It spanned approximately one hundred and twenty-five years through the dynasties VI to XII (c.2181–2055 BC). Tombs of this mysterious dark era were famous of including the models of ancient Egyptian daily-life. Copper-based tools such as chisels, axes, adzes were used as the principal tools for the ancient Egyptian craftsmen, artists, sculptors, carpenters, masons, quarry workers….etc (Driessen 1984; Evely 1992). So, due to the importance of the copper tools and the ancient Egyptian beliefs of resurrection and eternity, they buried their essential copper tools in their tombs for the worldly afterlife (Odler 2015). While, for uncertain reasons the ancient Egyptian craftsman resorted to manufacture small models for different daily-life features and put them in the elite burial's tombs of the old Kingdom. Thus, the copper model tools were usually as a part of funeral furniture in the tombs of the kings, queens, princesses and important official's persons. Older (Odler 2016) presented different suggestions to explain the purpose of existence of these copper model tools in the ancient Egyptian elites tombs. One of these suggestions explained that the copper model tools were most probably symbol of the patron–craftsman relationship. So, its existence is proof of the tomb's patron was so rich. While, the other suggestion is the ancient craftsmen might be kept the original tools and replaced them by small models which simulated to the original ones in the material and shape. There are previous studies investigated the microstructure, metal core, corrosion patina morphology/stratigraphy, corrosion mechanism, and treatment processes of the old kingdom's copper artifacts (Rademakers *et al*. 2018; Ibrahim & Maher 2018). While, little of these studies interested in study of copper modal tools especially that date back to the old kingdom and/or the first intermediate period (Odler & Dulíková 2015; Kmošek *et al*. 2016; Maher & Salem 2021). This work presented the morphology of the corrosion products, stratigraphy, and composition of hammered copper model tools dated back to Xth dynasty from Cairo Egyptian Museum collection. The study was performed by using different microscopies and multianalytical procedures to investigate the case-study artifacts'. Finally, the study introduced suitable treatment/conservation/display strategies for the case-study set or other such cases.

Materials and methods

The case-study is a copper model tools set from Cairo Egyptian Museum collection [Figure 1]. The set was discovered among the beads that were laid in a heap below the chest of the west coffin in the TOMB OF KHENNU AND APA-EM-SA-F (289). KHENNU AND APA-EM-SA-F tomb dated back to the Dynasty Xth, 1st Intermediate Period (c.2134-2050 BC). The KHENNU AND APA-EM-SA-F tomb is located in the south of Memphis (Saqqara), and it was excavated by Quibell in (1906-1907) (Quibell 1908). Firstly, the set was registered by excavation number (507), and then it was enrolled under the registration number JE39230 in Cairo Egyptian museum's archives. The set consists of twenty-five objects "three axes, fourteen chisels, seven adzes, and one dead-end needle". Table 1 shows a list of the identification name, dimensions, weights, corrosion description of the set objects, and the performed analysis procedures on each object. The set was badly stored inside a carton box in base 1, pup.3 of the showcase L in the room 32 at the upper floor of the museum [Figure 2]. Visual examination revealed that all the set objects suffer from severe corrosion products with different degrees and sandy-soil residues. Fortunately, it's the first time the set will be undergoing a study; this gives authenticity to all taken samples.

Different microscopes were used to examine the morphology and stratigraphy of corrosion layers. Dnt DigiMicro Mobile USB/TT Portable Digital Stereomicroscope 500X, 5.0 Megapixel was used to examine the outer-surface corrosion products on all the objects. Metallographic microscope was used to investigate the microstructure of the remaining metal core. This was performed via computerized optical light microscope model Olympus BX41M attached with a digital video camera. Three small samples (3×3 mm) were cut off the chisels (E, I) and adze (R) by using a jewelry saw (Figure 1 - dashed lines indicate the locations of the samples). The cross-sections samples were prepared to the microscopic examination by fixing in epoxy resin, and then polished by different coarseness emery papers (800–4000 grit) and diamond paste (1-3 µm). Polishing process is very important to obtain a smooth cross-section surface suitable to the metallographic examination. Polished cross-sections were examined before and after treated by diluted solution from alcoholic ferric chloride etching. Since, this etching solution attacked the oxide inclusions only and eventually the metal grain structure becomes

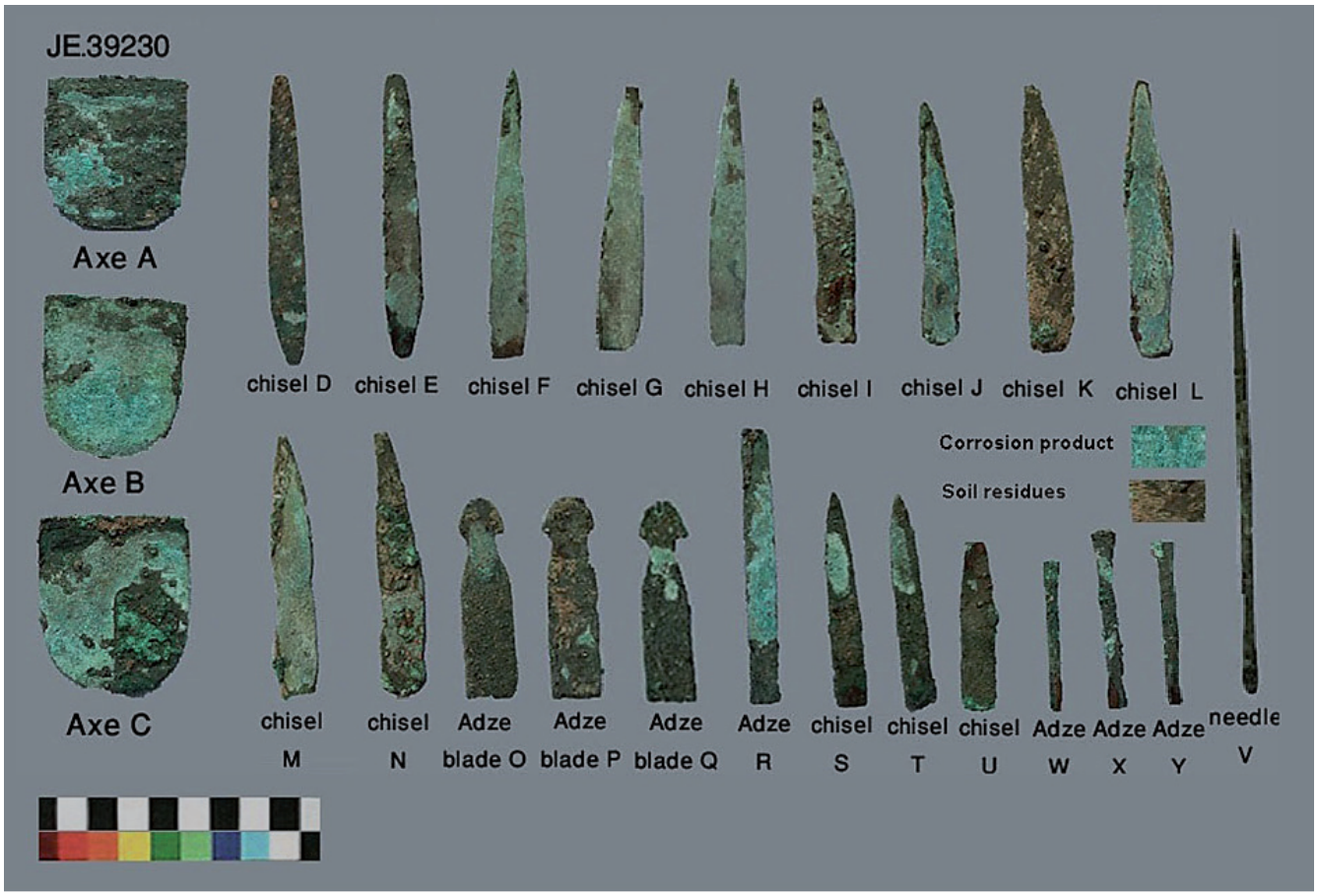

Figure 1.- Case-study set of the copper model tools; dashed lines and arrows point out the samples locations

visible (Scott 1991). Scanning Electron Microscope attached with Energy-Dispersive X-ray Spectroscopy (SEM-EDS) was performed to analyze the elemental composition of the remaining metallic core and corrosion product layers. The examination was carried out on SEM-EDS apparatus Model FEI INSPECT S50, EDS Quantax Bruker. The polished cross-sections were examined without coating. The analysis was performed under low vacuum mode at 0.8 torr. Backscatter electron images (BSE) were gotten at acceleration voltage 25.0 kV with a backscattered detector at 5 mm working distance and spot size 6. X-ray diffraction was used to investigation the chemical composition of the outer-surface corrosion products. Three powder samples were scraped off parallel to the surface of the chisels (E, I) and adze (R) [Figure 1- red arrows pointed out the locations of scraped off samples]. The samples were grinded in an agate mortar to be a very fine powder. The samples were analyzed via XRD equipment PAN analytical X'pert PRO Diffractometer model. The analysis was performed under experimental conditions as follow: secondary monochromator with a Cu-Kα1 target of λ 0.1542 nm, operated at generator power 45 kV and 40 mA, the scanning steps rate and range were 0.02°, 0.05°/s, and 70° respectively. 2θ values and relative intensities (I/Io) were determined and the resulted minerals were identified via JCPDS (Joint Committee for Powder Diffraction Studies) and AMCSD (American Mineralogist Crystal Structure Database) cards.

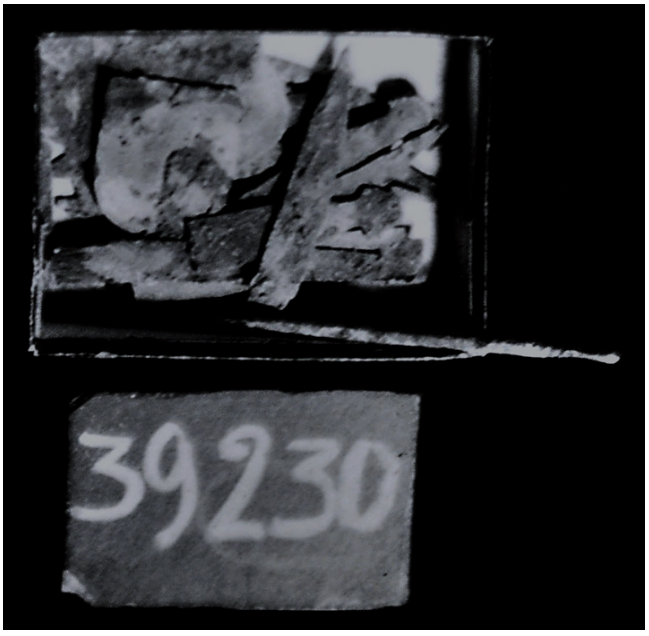

Figure 2.- Archival photograph of the case-study set during its storage in case L - base 1 - pup 3 in room 32, Cairo Egyptian Museum

Raman spectroscopy was used to study the micro-stratigraphic of the inner-corrosion layers in the cross-sections and hence identify its chemical composition. Raman spectroscopy is an ideal technique for the

Table 1.- List of twenty-five objects of the case-study set illustrates its identification name, dimensions, weight, corrosion description, and the performed analysis procedures

Serial	Object identification	Length (mm)	Width (mm)	Thickness (mm)	Weight (g)	Corrosion Description	Analysis*
A	Axe	2.6	2.3	≈ 1	0.53	Week adherent blue, pale green and solid dark green agglomerated corrosion products. Sandy-brown soil residues sometimes mixed with the corrosion products, while on some object it takes a flaking impact.	OM
B	Axe	2.6	2.3	≈ 1	0.53		OM
C	Axe	2.6	2.3	≈ 1	0.53		OM
D	Chisel	5.7	0.8	≈ 1	0.40		OM
E	Chisel	5.4	0.7	≈ 1	0.33		OM, XRD, SEM-EDS, Raman
F	Chisel	5.7	0.7	≈ 1	0.36		OM
G	Chisel	4.6	0.9	≈ 1	0.37		OM
H	Chisel	4.7	0.8	≈ 1	0.34		OM
I	Chisel	5.0	0.7	≈ 1	0.31		OM, XRD, SEM-EDS, Raman
J	Chisel	4.6	0.7	≈ 1	0.29		OM, XRD, SEM-EDS
K	Chisel	4.4	0.8	≈ 1	0.32		OM
L	Chisel	4.2	0.9	≈ 1	0.38		OM
M	Chisel	4.3	0.8	≈ 1	0.31		OM
N	Chisel	4.0	0.6	≈ 1	0.22		OM
O	Adze blade	3.7	1.0	≈ 1	0.33		OM
P	Adze blade	3.7	0.9	≈ 1	0.30		OM
Q	Adze blade	3.6	0.9	≈ 1	0.29		OM
R	Adze	4.4	0.5	≈ 1	0.20		OM, XRD
S	Chisel	3.3	0.5	≈ 1	0.15		OM
T	Chisel	3.0	0.5	≈ 1	0.13		OM
U	Chisel	2.9	0.6	≈ 1	0.16		OM
V	dead-end needle	9.5	--	0.5	0.67		OM
W	Adze	3.5	0.3	≈ 1	0.30		OM
X	Adze	3.6	0.3	≈ 1	0.33		OM
Y	Adze	2.9	0.3	≈ 1	0.31		OM

* OM: Metallographic optical microscope, XRD: X-ray Diffraction; SEM-EDS: Scanning Electron Microscope with X-Ray Energy Dispersive analysis

investigation the metals patinas and inner corrosion layers (Bellot-Gurlet, L., *et al*. 2009). Raman measurements were carried out at room temperature by using dispersive Raman microscope model Senterra produce of Bruker Company. Spectra were acquired with a wavelength of 785 nm, laser power 25 MW, and aperture setting 50×1000 µm. The cross-sections were scanned twice and the spectrometer calibration was obtained from a silicon crystal in which the Raman signal is at 520.5 cm^{-1}.

Results and discusion

Morphology and micro-startifaction stracture

—*Portable digital steromicroscope*

A portable digital stereomicroscope was used to investigate the external corrosion layer. Figure 3 (a-j) shows different copper corrosion products and soil residues on the studied objects' surfaces. The pale blue color corrosion is the main corrosion product on the most studied objects and this phase was weakly adherent and easily scraped off whether during the sampling or treatment processes [figure 3 a, b]. The dark green corrosion covers the objects G, J, V, Y, X, W, U, and some areas on other objects. This dark green corrosion phase is strongly adherent, agglomerated on the objects' surfaces and difficulty scraped off during the sampling and treatment processes [figure 3 c, d]. Additionally, the pale green corrosion is the main corrosion product on the objects R, W, P, and on some areas on other objects [figure 3 e, f]. The reddish-brown corrosion appears above the green and blue corrosion layers on the surface of the axe B [Figure 3g]. Sandy-brown soil residues appear on all the set objects which sometimes take a flaking shape as appeared on the adzes X, Y surfaces (Figure 3 h), and sometimes it was incorporated with the green and blue corrosion products and sometimes take a massive granular lumps which is obviously on the surface of the axe C and the chisel K [figure 3 i, j].

— Metallographic microscope

Generally, the metallographic examination elucidated the internal structure of metals and the relationship between the inclusions and the matrix. Three samples were cut off the objects (E, I, R) and prepared as polished cross-sections for the microscopic examinations. To examine the microstructure of these cross-sections, it must be studied before and after treated with a freshly prepared etching solution of alcoholic ferric chloride in ethyl alcohol. Figure 4-I shows the stratification structure of the studied cross-sections consecutively (a) the outer corrosion layer, (b) the original surface, (c) the under-surface corrosion layer, (d) the metallic structure remnants, (e) the internal corrosion products within the metallic structure, (f) the sandy-soil residues and quartz grains in the outer corrosion layer. Figure 4-II (a, b, c) shows the elongation of metal grains indicating to the direction of hammering process. Also, it is obvious high deformation of metal grains with a lot of strain lines and relatively coarse structure of the metal grains. This high deformation is due to the heavy working of the objects which entirely obliterated the initial segregated sponge-cored structure of the metal. The Figure also shows an intergranular corrosion through the strain lines (slip bands) which is resulted to the hammering process for the objects manufacture. Logically, the stress corrosion is formed due to the progressive nucleation and growth of the localized corrosion along the grain's boundaries around the metal grains especially in the presence of the moisture and oxygen as corrosion conditions (King, A. *et al.* 2008). Figure 4-II (d, e) shows the twins, which it is existence indicate to hammering and annealing cycles during the manufacture of the objects. The annealing process is a very important procedure during the hammering process, since it was performed at high temperatures for many hours prior to the striking the object. Abundance of strain lines and littleness of the twins indicate to the extensive cold-worked which did not follow up by sufficient annealing time especially in the final stage of the objects manufacture (Scott 1991).

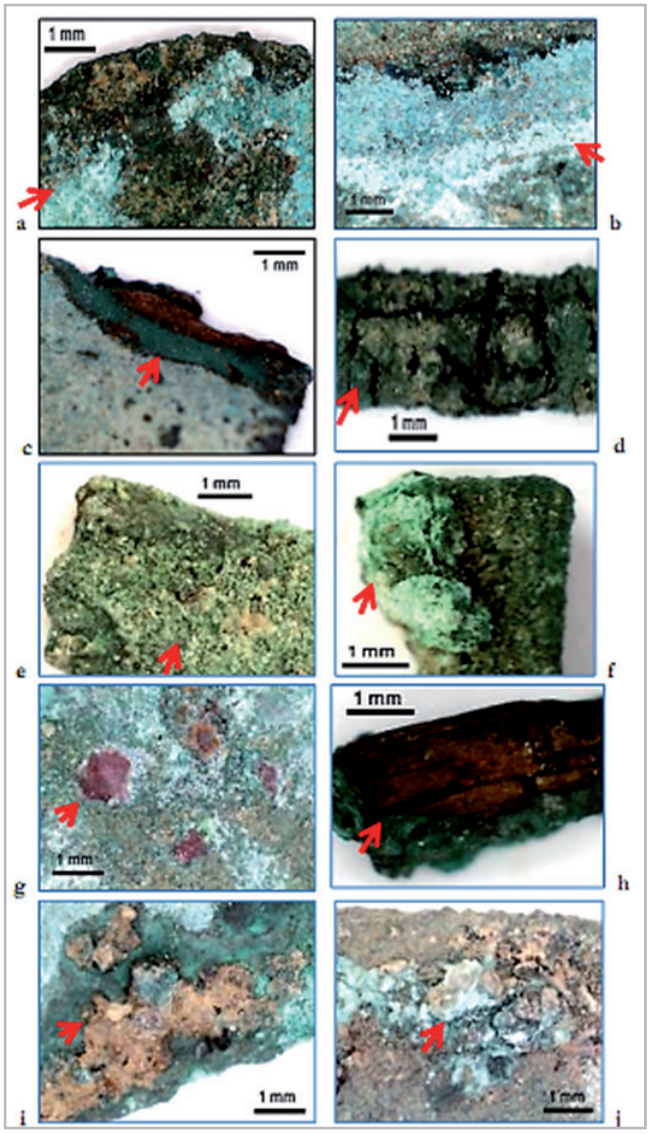

Figure 3.- Portable Stereomicroscope micrographs show different copper corrosion products: (a, b) pale blue corrosion on the surface of the chisel's J and U; (c, d) dark green corrosion on the surface of the chisel's G and J; (e, f) pale green corrosion on the surface of R and W adzes; (G) reddish-brown corrosion on the surface of axe B ; (h) flaking sandy-brown soil residues on the surface of the adze X ; (i, j) massive granular lumps of soil residues mixed with green corrosion products on the axe C and chisel K surfaces.

— Scanning electron microscope-energy dispresive X-ray

Essentially SEM-EDS were performed to identify the elemental composition of the metal core and the corrosion products in different layers of the studied cross-sections. Table 2 shows EDS' elemental analysis of the three objects E, I, R respectively. Figure 5 (I-III) shows the back-scattered SEM micrographs and EDS patterns through different layers of the objects (E, I, R) respectively.

EDS' results show the studied cross-sections' metal-cores consist only of copper without any alloying element [spots (E1, I1, R1-3]. Also, EDS' results show the presence of the elements Cu, C, O, Cl, S, Si, Mg, Ca, Al, Fe through different layers of the studied cross-sections. Since, the presence of O, Cl, C, and S elements are due to the formation of copper oxides, chlorides, basic carbonate, sulfides and/or sulfates corrosion products. EDS' analyses show an increase of the carbon percentage than the chlorine in all spots. It is high probability this increase indicates to the existence of copper carbonates as major corrosion products while the copper chlorides as minor. Since, EDS' analyses shows high percentage of chlorine in the outer corrosion layer in values 13.95 %, 11.72 % in the chisels E, I respectively [Table 2, spots E4, I3]. While, its presence in the metallic cores appears in values 0.67%, 1.67%, and 17.85% respectively [Table 2, spots E1, I1, R2]. The presence of chlorine element in the metal cores indicates to attack the studied objects by bronze disease. Additionally, BSED micrographs show

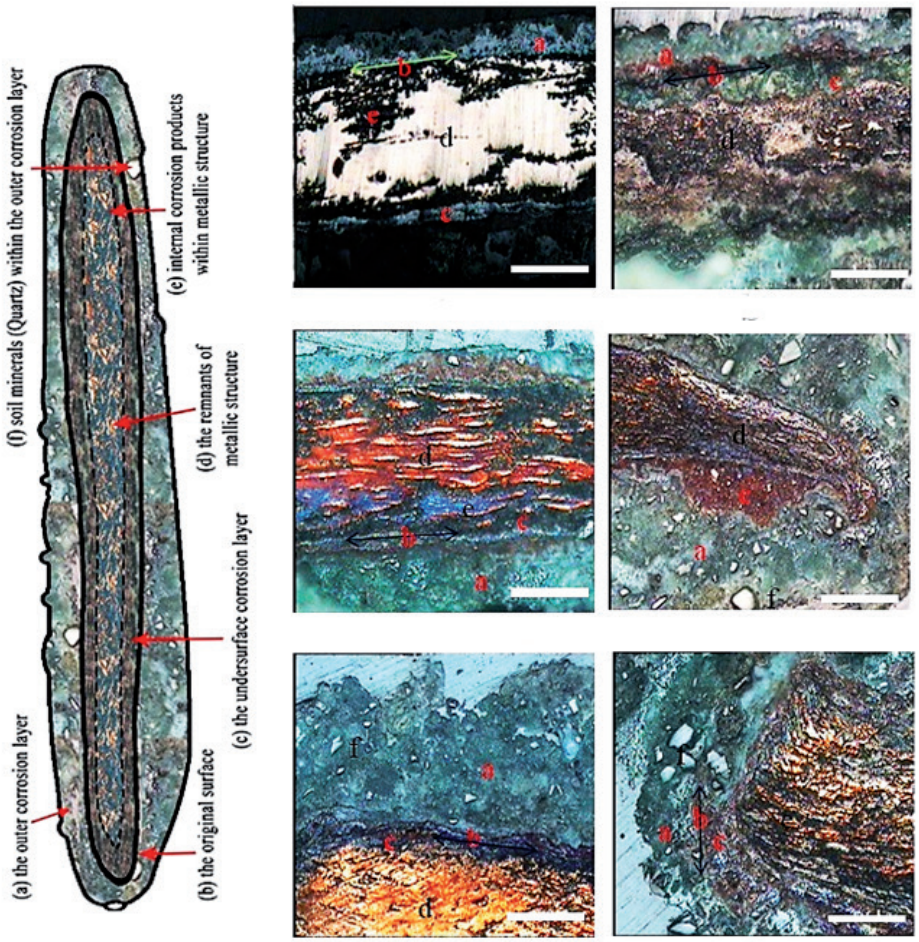

Figure 4.- I. Metallographic micrographs of the three cross-sections from the chisels E (a-c), I (d-e), and adze R (f) respectively before and after applied etching solution. Schematic description of the corrosion layers consecutively: (a) the outer corrosion layer, (b) the original surface, (c) the under-surface corrosion layer, (d) the metallic structure remnants, (e) the internal corrosion products within the metallic structure, (f) the sandy-soil residues and quartz grains which in the outer corrosion layer

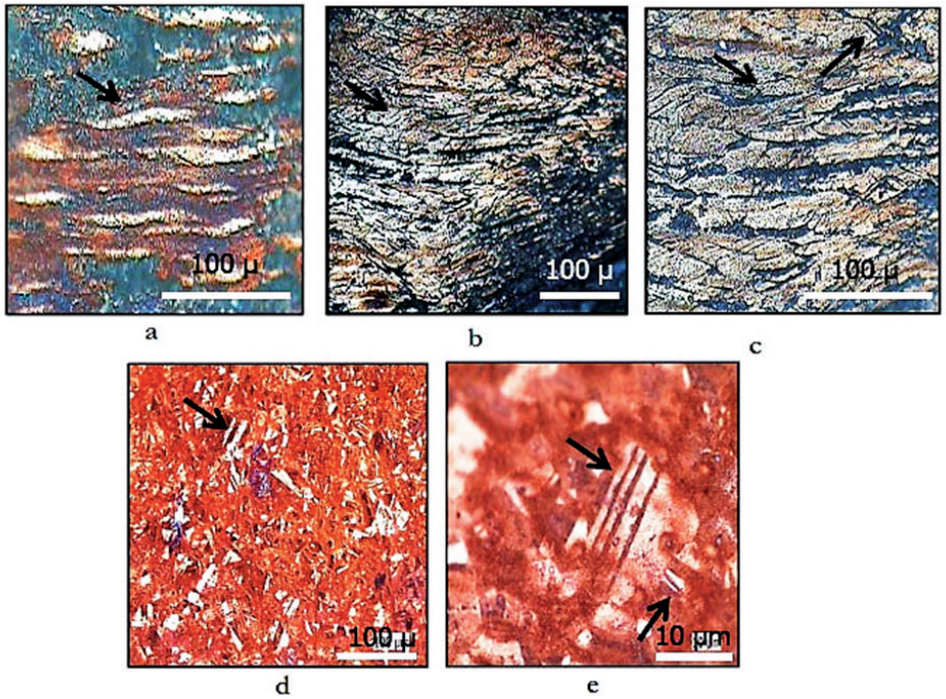

Figure 4.- II (a, b, c) the elongation of individual metal grains parallel to flat surfaces of the hammered chisels; (d, e) the twins as a result of the hammering and annealing cycles during the manufacture of the set objects

Table 2.- EDS' analysis results of the cross-sections from the objects E, I, R respectively

Object symbol	Spot	Sample Description	Cu	C	O	Cl	S	Si	Mg	Ca	Al	Fe
Chisel E	1	Metallic core	84.91	12.75	1.57	0.67	0.00	0.10	0.00	0.00	0.00	0.00
	2	The outer corrosion layer	42.01	26.36	18.35	11.24	0.00	0.44	0.76	0.56	0.27	0.00
	3	The under-surface corrosion layer	61.39	19.08	8.10	6.54	4.89	0.00	0.00	0.00	0.00	0.00
	4	The outer corrosion layer	43.36	18.31	24.40	13.95	0.00	0.00	0.00	0.00	0.00	0.00
Chisel I	1	Metallic core	98.33	0.00	0.00	1.67	0.00	0.00	0.00	0.00	0.00	0.00
	2	The under-surface corrosion layer	67.20	15.14	15.42	2.24	0.00	0.00	0.00	0.00	0.00	0.00
	3	The outer corrosion layer	54.18	20.48	10.71	11.72	0.00	1.83	0.00	0.00	0.55	0.54
Adze R	1	Metallic core	74.31	11.60	11.04	3.05	0.00	0.00	0.00	0.00	0.00	0.00
	2		54.34	18.75	9.06	17.85	0.00	0.00	0.00	0.00	0.00	0.00
	3		84.17	12.02	2.46	1.34	0.00	0.00	0.00	0.00	0.00	0.00
	4	The inner corrosion layer	48.75	14.72	22.00	14.54	0.00	0.00	0.00	0.00	0.00	0.00

the existence of an under-surface corrosion layer between the outer corrosion crust and remnants of the metallic core which also contains a high percentage of chlorine. The chlorine presents through this under-surface layer in values 6.54 %, 2.24 %, 14.54 % respectively [table 2, spots E3, I2, R4]. The existence of oxygen indicates to the presence of copper oxides corrosion products such as reddish-brown corrosion product which appears on the surface of the axe B. Finally, the existence of Si in the outer corrosion layer indicated to the presence of quartz as a confirmation to the initial buried environment of the studied objects is sandy soil [table 2, spots E2, I3]. The presence of Mg, Ca, Al, Fe elements also indicates to presence of clay components in the buried soil. Generally, the microscopic examinations of the cross-sections of the chisels E, I, and adze R show a multilayered corrosion structure of three layers as follows: an outer corrosion layer which contains sandy-soil residues and quartz grains followed by an under-surface layer, then an internal layer within the metallic structure.

Chracterization of corrosion products

— *X-ray diffraction*

X-ray diffraction was used to identify the chemical composition of powder corrosion products samples. The identification was achieved by matching the samples d-spacing values with JCPDS and AMCSD cards. Figure 6 (a-c) and Table 3 show XRD patterns and the results of three corrosion samples which were scraped off the surfaces of the objects E, I, R respectively. XRD results show the samples consist of copper oxides, chlorides and basic carbonates. These corrosion products are commonly identified on most of the ancient copper-based alloys. Cuprite [JCPDS cards (071-4310), (05-0667)] was detected in the three samples. Copper chlorides were detected with various phases; paratacamite [JCPDS card (025-1427)] was detected in the chisel E sample; atacamite [JCPDS cards (078-03772), (23-948)] and Nantokite [JCPDS cards (082-2117), (06-0344)] in the samples of the objects I, R. The pale blue copper chloride corrosion product "Bronze disease" is common on most ancient copper-based alloys due to the presence of chlorides ions in the Egyptian soils (Scott 1990). The green and dark green copper carbonates corrosion products malachite [(AMCSD 0009305), JCPDS (10-0399) cards] was detected in the samples of the objects E, R; while chalconatronite [JCPDS (10-442), AMCSD (0010801 cards] was detected in the chisel E sample. Finally, quartz [AMCSD card (00110099)] was detected in the chisel I sample. The existence of quartz was explained due to the soil residues which were mixed with the outer corrosion layer.

— *Raman spectroscopy*

Raman spectroscopy was used to identify the chemical composition of under-surface and internal corrosion layers. The results show the presence of atacamite ($Cu_2(OH)_3Cl_2$ and malachite ($Cu_2(OH)_2CO_3$) corrosion products. Figure 7 shows Raman patterns of atacamite and its micrograph in the under-surface corrosion layer of the chisel I. Also, it shows Raman pattern of malachite corrosion and its micrograph in the internal corrosion layer through the metallic structure of the chisel E. Malachite shows a very intensive strong band at the wavenumber 271 cm^{-1} which is represented its finger print, in addition its actualization in other secondary bands at the wavenumbers 144, 340, 545, 811 and 1052 cm^{-1} (Zhang *et al.* 2014; Inberg *et al.* 2018, Łukasz Ciupiński, 2010, Frost R L. 2002; Daniel Cosano 2018). While, atacamite exhibits strong Raman bands at wavenumbers 511, 3460, 3320 cm^{-1}, in addition its actualization at the wavenumbers 820, 890 and 985 cm^{-1} (Frost *et al.* 2002; Frost 2003; Bertolotti 2012; Ropret 2012; Schindelholz 2018). This is besides its matching with the equipment library standard as shown in the Figure 7-b. Cuprite is a usual corrosion product on the copper-based

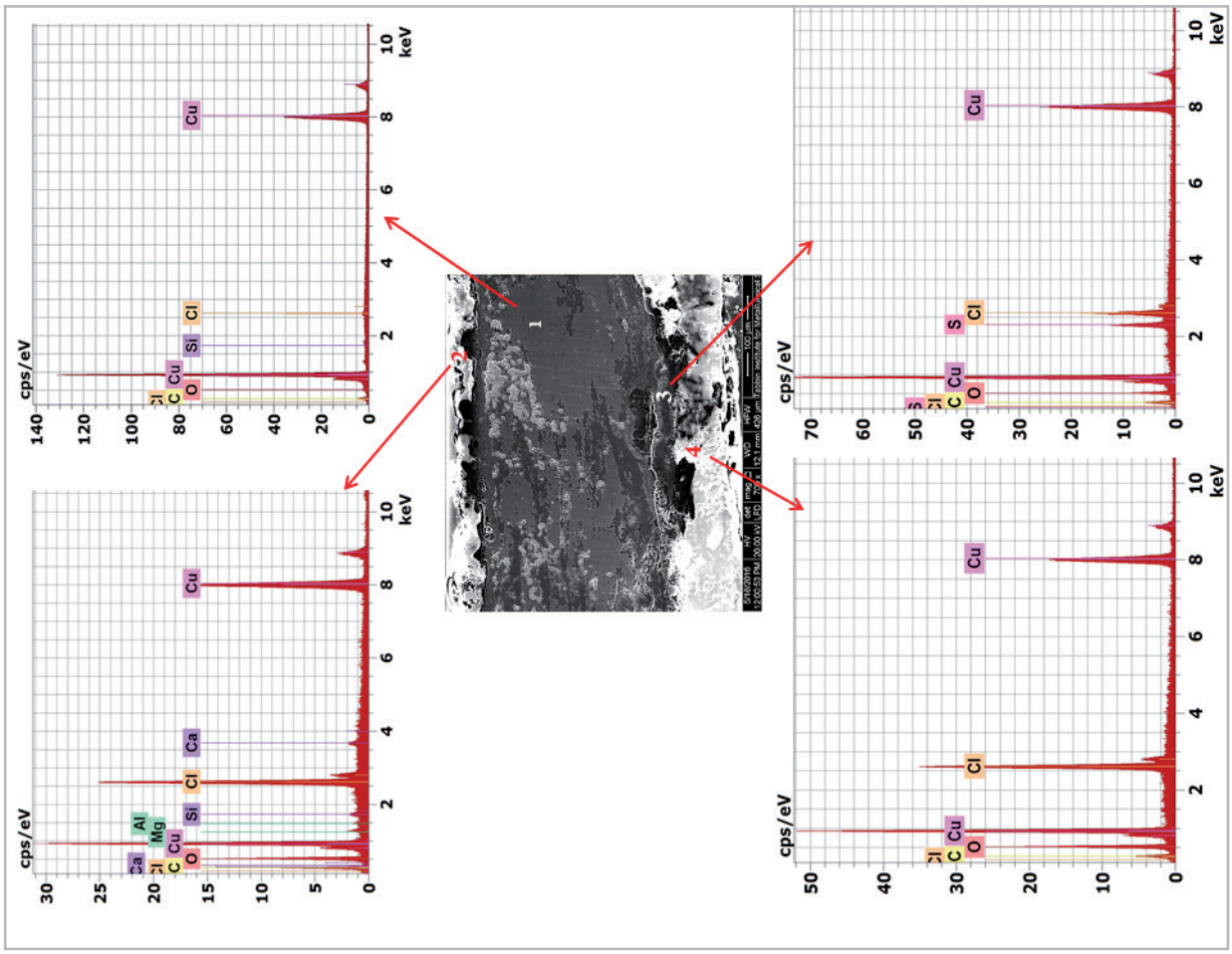

Figure 5.-I. SEM-EDS of different stratification layers of the cross-section of the chisel E

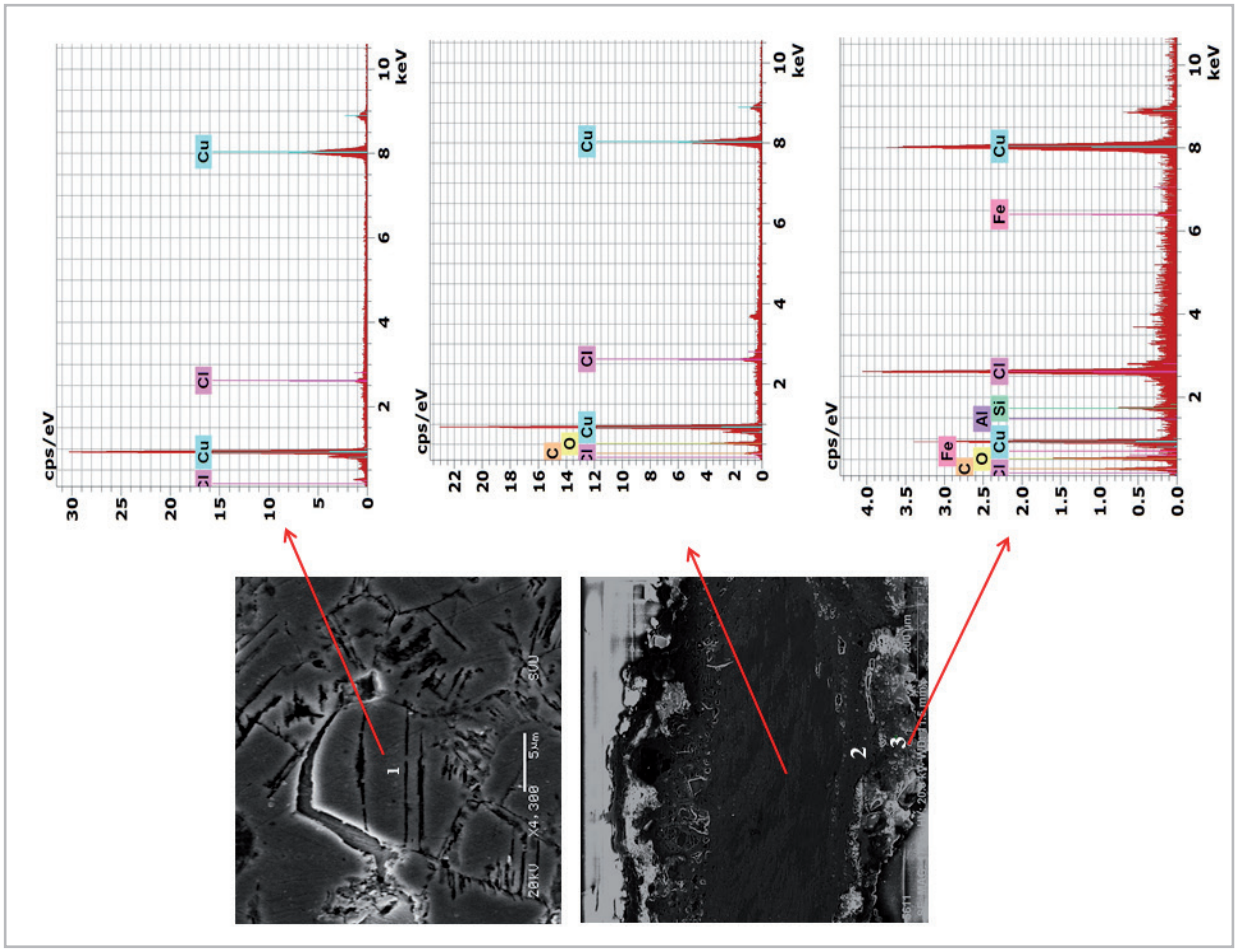

Figure 5.-II. SEM-EDS of different stratification layers of the cross-section of the chisel I.

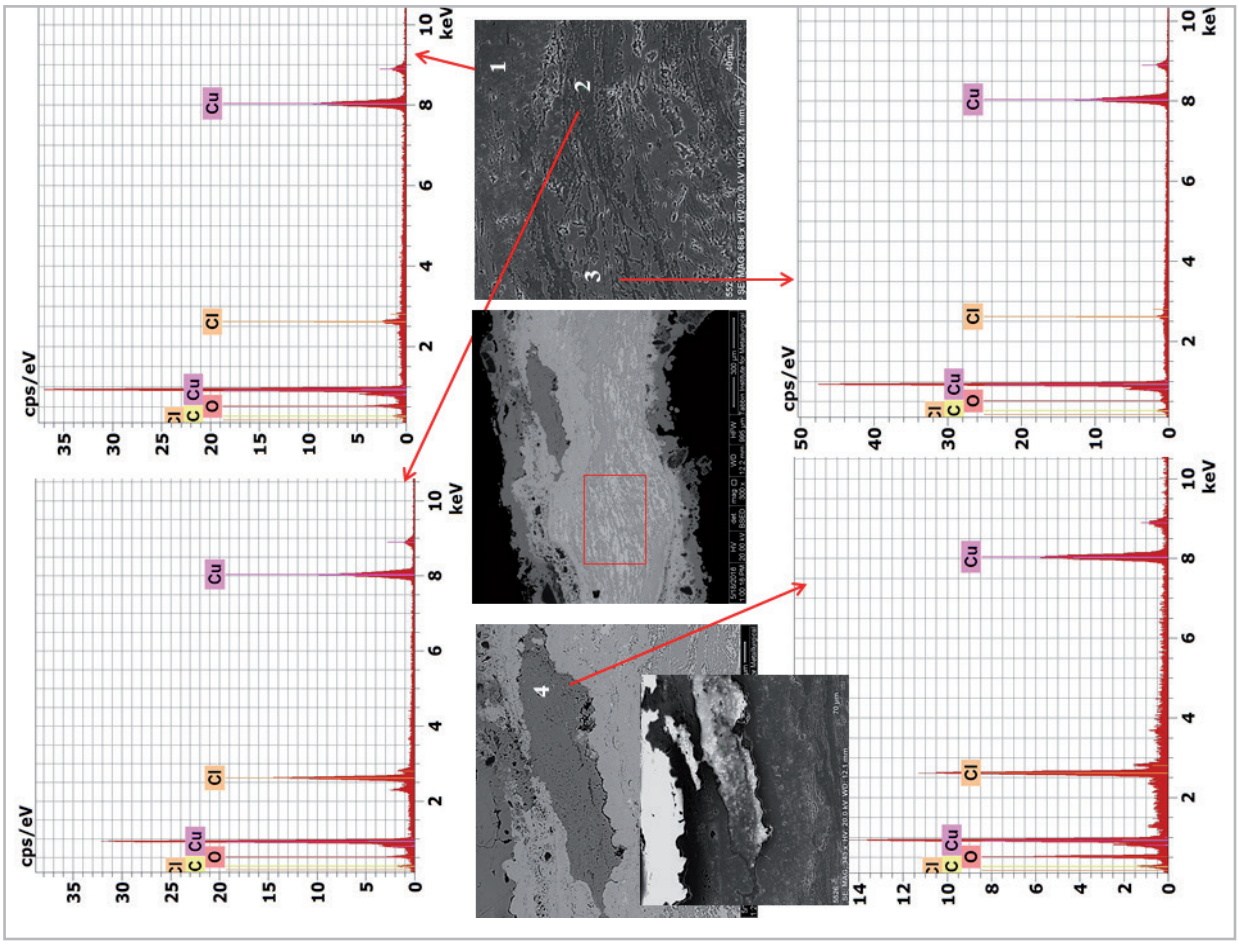

Figure 5.-III. SEM-EDS of different stratification layers of the cross-section of adze R.

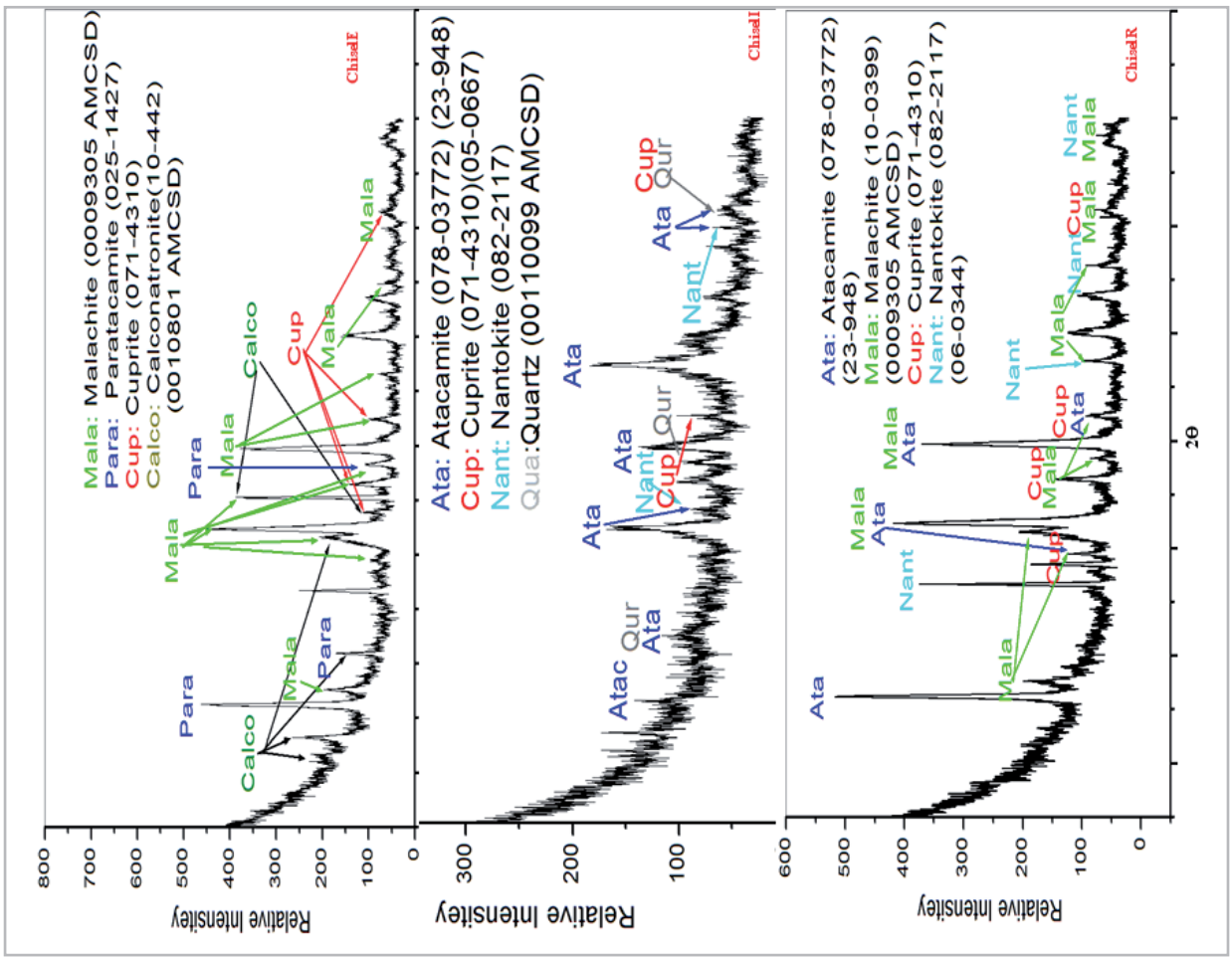

Figure 6.-(a-c). XRD patterns of the three powder corrosion samples scraped off the objects E, I, R respectively

Table 3.- . XRD analysis results of the three powder corrosion samples scraped off the objects E, I, R respectively

Object symbol	cuprite Cu_2O	paratacamite $Cu_2(OH)_3Cl$	nantokite CuCl	atacamite $Cu_2(OH)_3Cl$	malachite $CuCO_3.Cu(OH)_2$	chalconatronite $Na_2Cu(CO_3)_2.3(H_2O)$	quartz SiO_2
Chisel E	+	+			+	+	
Chisel I	+		+	+			+
Adze R	+		+	+	+		

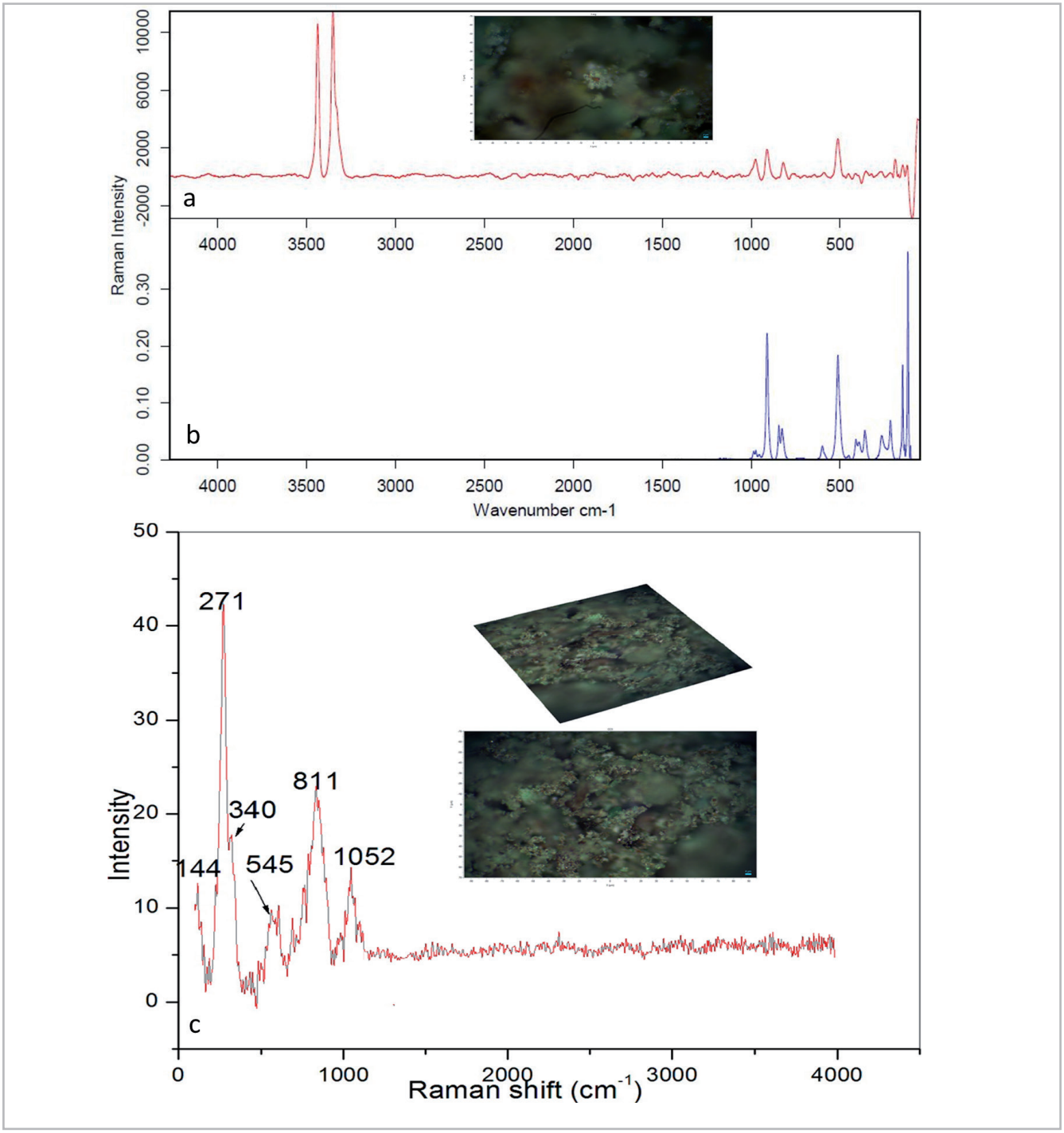

Figure 7.- (a,b) Raman pattern and micrograph of atacamite in the under-surface corrosion layer of the chisel I matched with equipment library standard; (C) Raman pattern and micrograph of malachite in the internal corrosion layer through the metallic structure of the chisel E

artifacts; since it can form as an original corrosion layer due to the direct chemical reaction between the copper and the oxygen during the long burial time (FitzGerald *et al.* 2006). Nantokite often can form on the copper-based artifacts as an original corrosion product due to the direct reaction between the chlorines ions and the cuprous corrosion (Strandberg & Johansson 1998). Also, it can form as a secondary product due to dissolution of cuprite corrosion in the presence of high humidity, oxygen and chlorines in the surrounded environments (Fitzgerald *et al.* 1998).

XRD results detected also atacamite and paratacamite corrosion products as basic copper chloride isomers. Atacamite can form as an original corrosion product whether during the burial or storage time due to the direct chemical reaction between the chlorines and the dissolved copper ions. Additionally, it can form as a secondary product as result to transformation of nantokite and cuprite in the existence of chlorine ions, high humidity, and oxygen in the storage environment (Strandberg & Johansson 1998). While, paratacamite usually appeared as an outer secondary corrosion layer in a powdery pale blue corrosion product on other corrosion layers (Scott 2002). Additionally, the formation of paratacamite can be attributed also as a result to the conversion of nantokite in the presence of high humidity and the oxygen. Also, it can form due to the transformation of an unstable atacamite isomer in the presence of high humidity and the oxygen (Krätschmer *et al.* 2002; Zhang *et al.* 2014). Thus, all these suggestions of the formation the nantokite, atacamite, and paratacamite on the case-study set are acceptable. Whereas, this transformation process can be facilitated due to increase of the porosity and cracking in the outer corrosion layers [See Figure 3 d]. Since, this cracking in the outer corrosion layer ease the penetration of the moisture and the oxygen into the internal metal core and thus formation the under-surface and internal corrosion layer which will be increase the corrosion rate of the studied objects (Krätschmer *et al.* 2002). Malachite usually can form above the initial cuprite layer due to the direct chemical reaction of the carbonate/bicarbonate anions and the copper and/or cuprous oxide patina in the presence of the high humid environment (Vink 1986). The carbonate/bicarbonate anions can be resulted due to the dissolution of the salts through the buried soils. Malachite can form also due to the presence of carbon dioxide gas in humid air (He, L., *et al.* 2011). Additionally, EDS' results indicated to increase of carbon than chlorines ions [Table 2]; this can be explained due to the presence of the carbonate corrosion as the main corrosion products than the chlorides in the remaining metallic structure. Also, Raman measurements confirmed the existence of atacamite and malachite corrosion products in the internal corrosion layers of the studied cross-sections.

Finally, the formation of various corrosion products on the case-study set can be explained due to not only the long-burial time in the tomb but also due to the uncontrolled storage conditions after its excavation and transportation to the museum.

Since, the set was exposed to indirect burial conditions in the tomb's burial chamber for a long time in an equilibrium condition. Then after its excavation and transportation to the museum, it was exposed to uncontrolled humid storage environment for more than 110 years. During this long storage time, the objects were stored in a carton box [See figure 2]. This bad storage conditions facilitated the corrosion process of the set objects especially when the relative humidity increased. Whereas, the most museums' halls doesn't prepare with a central air condition or air filters in order to preventing the pollution gases and the solid pollutants from the outdoor source. Additionally, since the late of seventies the museum's halls were covered with gray and black vulcanization rubber slabs, which is represented the main indoor source of pollution gases [(Maher & Salem 2021)]. Thus, the uncontrolled storage condition is the main cause of the resulted progressive morphologies and layered structure of the corrosion products and the partial mineralization for all set objects.

Treatment and conservation

Firstly, the case-study set was cleaned mechanically by using dental vibrotools and different coarseness carborundum 'Silicon carbide (SiC)' vibrotools' heads according to the hardness of corrosion layers. Sometimes, the dental ultrasonic scaler was used to clean the bronze disease spots. After finishing the mechanical cleaning, the set was treated with a corrosion inhibitor benzotriazole 3% in ethanol alcohol then coated by Paraloid B72 3% in acetone. To assess the effectiveness of pervious treatment processes, the set was put in a closed environment containing a high humidity source for three weeks. Unfortunately the pale green and dark green corrosion products emerged from the first day of the test especially in the bronze disease locations [figure 8 (a-c)]. So, the authors cleaned the set objects chemically to removing the emerged corrosion products. Then, the set was treated with 5% sodium carbonate in distilled water for 24 hours as a pre-treatment before applied the inhibitor and coating (Weisser & Black 1987). Figure 9 shows the success of this pre-treatment by sodium carbonate. After the treatment processes, the set was mechanically fixed on a Plexiglas plate by sewing technique with transparent inert plastic threads no.50 (Diameter 0.5 mm). Since, the use of plastic sewing threads is more suitable and safe for fixing the metal artifacts because it has good flexibility, especially at low temperatures. Since, this flexibility is very useful during the sewing process because it allows to stretching the threads without cutting-off, besides it has high tensile strength. More importantly, it has high corrosion resistance thus it is more suitable for fixing the metal artifacts. Also, it is characterized by good durability because it has excellent resistance against the abrasion, UV, and mildew. In addition, it is substantially inert against the alkalis and unaffected by most mineral acids (Anon 1968). Furthermore, it has good transparency/or semi-transparency thus it did not visible for the visitors.

Conclusion

The set of copper model tools dated to Dynasty Xth from Cairo Egyptian Museum were characterized and conserved. The multianalytical investigation results of the set give insight into its microstructure features, composition, and corrosion mechanism. EDS' showed that the chemical composition of the metal core of the analyzed objects consists of copper metal and didn't detect any alloying elements. The metallographic examination of the cross-sections showed features of metallic structures concerning a manufacturing process that was a hammering method. The microscopic investigation revealed elongation of metal grains which indicating to the direction of hammering process. Twins and strain lines are indicators to use sequential cycles of cold-working and annealing processes during the manufacture the case-study. The microscopic investigation revealed stratification structure of the corrosion as two sequence layers; an under surface layer followed by an outer thick layer. Besides, exist of internal corrosion products within the metallic structure in the center of the samples. The mechanism of corrosion products of the case-study was attributed to deterioration the case-study set during the burial time as well as due to

Figure 8.- (a) Photograph of the case-study set during RH test assessment; (b, c) stereomicroscope images of the emerged pale and dark green corrosion products due to exposure the set to high humidity

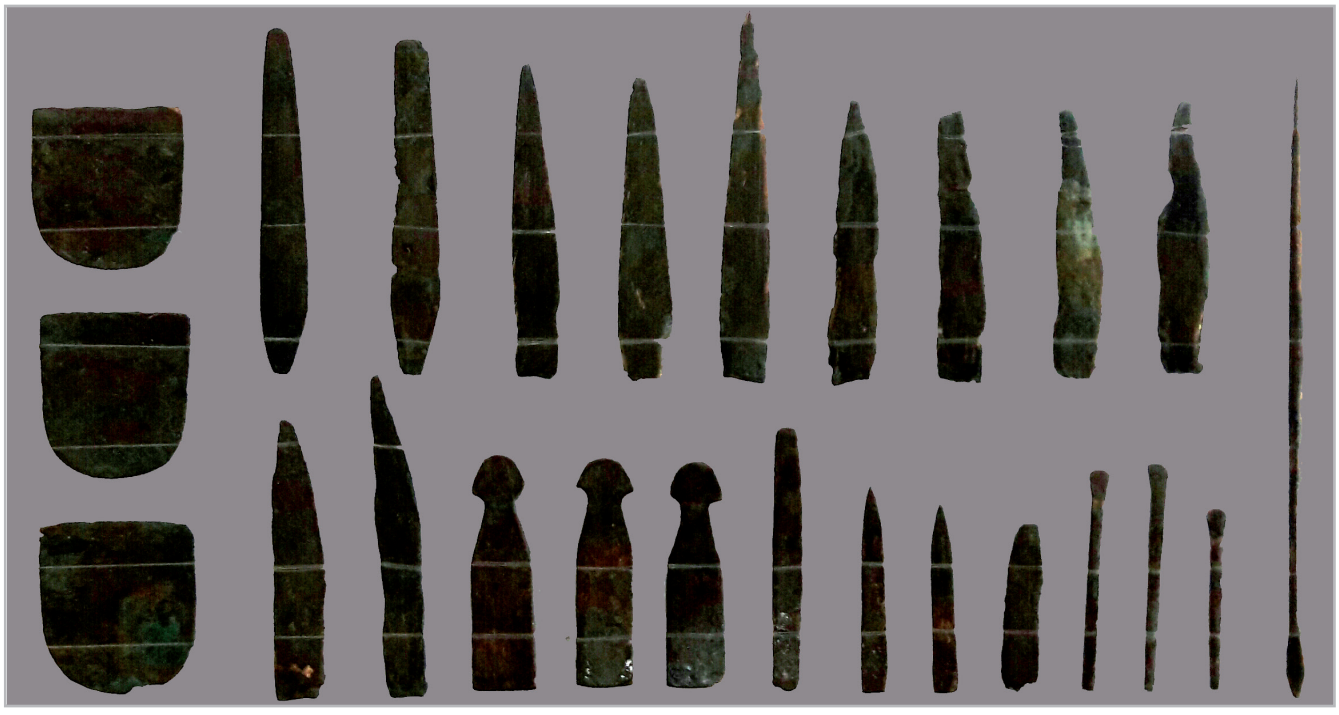

Figure 9.- . Photograph of the case-study set after treatment and fixing on a Plexiglas plate by transparent sewing threads

transformations of the corrosion phases during the long-term uncontrolled storage environment. X-ray diffraction and Raman spectroscopy confirmed that the corrosion products consist of a mixture of copper oxides, chlorides, and basic carbonates minerals. Additionally, the samples contain a certain portion of sand particles (quartz) which is an indicator of the burial soil type. Eventually, the set had been mechanically cleaned, pre-treated with 5% sodium carbonate in distilled water, then treated by diluted 3% Benzotriazole corrosion inhibitor in ethyl alcohol and coated by 3% Polaroid B72 in acetone. Finally, the set was fixed on Plexiglas plate by sewing technique via inert transparent plastic threads no.50 to be ready to display.

Acknowlegments

The authors acknowledge the valuable support given by Prof. M.A. Moustafa, X-head of Heat Treatment Department, Central Metallurgical R & D Institute (CMRDI) to help in the metallographic examination of the cross-sections. Also, they thank Dr. Gamal El-Balam the curator in the Cairo Egyptian Museum for his approval to investigation the case-study set.

References

ANON (1968). The World Book Encyclopedia Volume 7. s.l.: Field Enterprises Educational Corp.

BELLOT-GURLET, L., *et al*. (2009). Raman Studies of Corrosion Layers Formed on Archaeological Irons in Various Media. *Journal of Nano Research*, Issue 8: 147–156. https://doi.org/10.4028/www.scientific.net/JNanoR.8.147

BERTOLOTTI, G., BERSANI, D., LOTTICI, P.P., ALESIANI, M., MALCHEREK, T. AND SCHLÜTER, J. (2012). Micro-Raman study of copper hydroxychlorides and other corrosion products of bronze samples mimicking archaeological coins. *Analytical and bioanalytical chemistry*, 402(4): 1451-1457. https://doi.org/10.1007/s00216-011-5268-9

DANIEL COSANO, DOLORES ESQUIVEL, LAURA D. MATEOS, FERNANDO QUESADA, CÉSAR JIMÉNEZ-SANCHIDRIÁN, J. RAFAEL RUIZ (2018). Spectroscopic analysis of corrosion products in a bronze cauldron from the Late Iberian Iron Age. *Spectrochimica Acta* Part A: Molecular and Biomolecular Spectroscopy, Volume 205: 489–496.

DRIESSEN, J. (1984). Notes on building materials and quarries. In "An Archaeological Survey of the Roussolakkos Area at Palaikastro", Volume BSA 79, J.A. MacGillivray, L.H. Sackett, and J. Driessen, eds., 143–149

EVELY, D. (1992). "Stone Vases and Other objects". s.l.:In Well Built Mycenae, the Helleno-British Excavations within the Citadel at Mycenae, 1959-1969, Fasc. 27. Ground Stone. Part 1, edited by Don Evely and Curtis Runnels, 1 20. Oxford: Oxbow books.

FITZGERALD *et al.* (2006). Atmospheric corrosion of copper and the colour, structure and composition of natural patinas on copper. *Corrosion Science*,, 48(9): 2480-2509. https://doi.org/10.1016/j.corsci.2005.09.011

FITZGERALD, K. P., NAIM, J. & ATRENS, A. (1998). The chemistry of copper patination. *Corrosion science*, 40(12): 2029-2050. http://dx.doi.org/10.1016/S0010-938X(98)00093-6

FROST, R. L., MARTENS, W., KLOPROGGE, J. T. & WILLIAMS, P. A. (2002). "Raman spectroscopy of the basic copper chlorine minerals atacamite and paratacamite: implications for the study of copper, brass and bronze objects of archaeological significance". *Journal of Raman Spectroscopy*, 33(10): 801-806 https://doi.org/10.1002/jrs.921

FROST, R. (2003). Raman spectroscopy of selected copper minerals of significance in corrosion. *Spectrochimica acta* Part A: molecular and biomolecular spectroscopy, 59(6): 1195-1204 https://doi.org/10.1016/S1386-1425(02)00315-3

GETTENS, R. J. & FRONDEL, C. (1955). Chalconatronite: an alteration product on some ancient Egyptian bronzes. *Studies in Conservation*, 2(2): 64-75. https://doi.org/10.1179/sic.1955.009

HE, L., LIANG, J., ZHAO, X., & JIANG, B. (2011). "Corrosion behavior and morphological features of archeological bronze coins from ancient China". *Microchemical Journal* 99(2): 203-212. https://doi.org/10.1016/j.microc.2011.05.009

IBRAHIM A. G. & MAHER M. A. (2018). "A Case-study of Copper-Arsenic Ewer from the Egyptian Museum in Cairo, Egypt". *Journal of The General Union of Arab Archaeologists*, Volume (3), pp. 1-25. https://doi.org/10.21608/JGUAA2.2018.2766.1009

INBERG, A., *et al*. (2018). Corrosion products and microstructure of copper alloy coins from the Byzantine-period Ma'agan Mikhael B shipwreck, Israel. *Microchemical Journal,* Volume 143: 400-409. https://doi.org/10.1016/j.microc.2018.08.033

KING, A., JOHNSON, G., ENGELBERG, D., LUDWDIG, W., & MARROW, J. (2008). "Observations of intergranular stress corrosion cracking in a grain-mapped polycrysta". *Science*, 321(5887): 382-385. https://doi.org/10.1126/science.1156211

KMOŠEK J., *et al*. (2016). Archaeometallurgical study of copper alloy tools and model tools from the Old Kingdom necropolis at Giza, chapter in the volume "Old Kingdom copper tools and model tools". s.l.: Archaeopress Publishing Ltd., Oxford, 238-290. ISBN 978 1 78491 443 1 (e-Pdf)

KRÄTSCHMER, A., WALLINDER, I. O., & LEYGRAF, C. (2002). "The evolution of outdoor copper patina". *Corrosion Science*, 44(3): 425-450 https://doi.org/10.1016/S0010-938X(01)00081-6

MAHER, M.A. & SALEM, Y., 2021. An unusual corrosion product, kobyashevite, from ancient egyptian copper artifacts: a technicaL Note. *Egyptian Journal of Chemistry,* 64(1): 11 – 23. https://doi.org/10.21608/EJCHEM.2020.36950.2763

MARTENS, W., FROST, R. L., KLOPROGGE, J. T., & WILLIAMS, P. A. (2003). "Raman spectroscopic study of the basic copper sulfates implications for copper corrosion and 'bronze disease". *Journal of Raman Spectroscopy,* 34(2): 145-151. https://doi.org/10.1002/jrs.969

ODLER, M., & DULÍKOVÁ, V. (2015). "Social context of the Old Kingdom copper model tools". *World Archaeology*, 47(1): 94-116. https://doi.org/10.1080/00438243.2014.991805

ODLER, M. (2015). Adzes in the Early Dynastic period and the Old Kingdom, Conference Paper • January 2012 "Copper and Trade in the South–Eastern Mediterranean ,Trade routes of the Near East in Antiquity", Edited by Karolina Rosińska-Balik Agnieszka Ochał-Czarnowicz Marcin Czarnowicz Joanna Dębowska-Ludwin 85-109. ISBN 978 1 4073 1414 3

ODLER, M., (2016). *Old Kingdom copper tools and model tools.* s.l.: Archaeopress Publishing Ltd., Oxford. ISBN 9781784914431 (e-Pdf)

PEKOV, I. V., ZUBKOVA, N. V., YAPASKURT, V. O., BELAKOVSKIY, D. I., CHUKANOV, N. V., KASATKIN, A. V., & PUSHCHAROVSKY, D. Y. (2013). Kobyashevite, Cu5(SO4)2(OH)6•4H2O, a new devilline-group mineral from the Vishnevye Mountains, South Urals, Russia. Mineralogy and Petrology, 107(2): 201-210. https://doi.org/10.1007/s00710-012-0236-4

QUIBELL, J. E. (1908). *Excavations at Saqqara (1906-1907) with a section on the religious texts*. s.l.: Le caire: imprimerie de l'institut francais d'archeologie orientale. https://archive.org/details/excavationsatsaq1908quib

RADEMAKERS, F. W., VERLY, G., DELVAUX, L., & DEGRYSE, P. (2018). "Copper for the afterlife in pre Dynastic to Old Kingdom Egypt: provenance investigation by chemical and lead isotope analysis". (RMAH collection, Belgium). *J Archaeol Sci*., 96: 175-190. https://doi.org/10.1016/j.jas.2018.04.005

ROPRET P., K. T. (2012). Raman investigation of artificial patinas on recent bronze – Part I: climatic chamber exposure. J. *Raman Spectrosc*., 43: 1578–1586. https://doi.org/10.1002/jrs.4068

SCHINDELHOLZ E.J., CONG H., JOVE-COLON C.F., LI S., OHLHAUSEN J. A., MOFFAT H.K. (2018). Electrochemical aspects of copper atmospheric corrosion in the presence of sodium chloride. *Electrochimica Acta*, 276: 194-206. https://doi.org/10.1016/j.electacta.2018.04.184

SCOTT, D. A., (1990). "Bronze disease: a review of some chemical problems and the role of relative humidity". *Journal of the American Institute for Conservation* (JAIC), 29(2): 193-206. https://doi.org/10.1179/019713690806046064

SCOTT, D. A. (1991). *Metallographic and Microstructure of Ancient and Historic Metals* (No. 77). s.l.: Los Angeles, CA: The Getty Conservation Institute. ISBN 0-89236-195-6 (pbk.)

SCOTT, D. A. (2002). Copper and bronze in art: corrosion, colorants, conservation. s.l.: Getty publications. ISBN 0-89236-638- 9

STRANDBERG, H., & JOHANSSON, L. G. (1997). "Role of O3 in the atmospheric corrosion of copper in the presence of SO2". *Journal of the Electrochemical Society*, 144(7): 2334. https://iopscience.iop.org/article/10.1149/1.1837814/meta

STRANDBERG, H., & JOHANSSON, L. G. (1998). "Some aspects of the atmospheric corrosion of copper in the presence of sodium chlorine". *Journal of the Electrochemical Society*, 145(4): 1093-1100. https://iopscience.iop.org/article/10.1149/1.1838422

STRANDBERG, H., LANGER V., & JOHANSSON L.G. (1995). Structure of Cu2.5(OH)3SO4•2H2O: a Novel Corrosion Product of Copper. *Acta Chemica Scandinavica*, 49(1): 5-10. http://actachemscand.org/pdf/acta_vol_49_p0005-0010.pdf

VINK, B. W., (1986). "Stability relations of malachite and azurite". *Mineralogical Magazine*. 50(355): 41-47. https://doi.org/10.1017/minmag.1986.050.355.06

WEISSER, T. D., & BLACK, J. (1987). "The use of sodium carbonate as a pre-treatment for difficult-to-stabilise bronzes". London, In *Recent Advances in the Conservation and Analysis of Artifacts,* edited by J. Black, Summers Schools Press, 105-108.

ZHANG, X., WALLINDER, I. O., & LEYGRAF, C. (2014). "Mechanistic studies of corrosion product flaking on copper and copper-based alloys in marine environments". *Corrosion Science*, 85: 15-25. https://doi.org/10.1016/j.corsci.2014.03.028

Autor/es

Manal Ahmed Maher Abdel Raouf
manal.a.maher@gmail.com
Head of Computed Tomography X-Ray unit, Cairo Egyptian Museum, Ministry of Antiquities, Egypt.

Graduated from Faculty of Science; physics Dept. Ean-Shames University 1993. Gained a diploma of conservation science from conservation department, faculty of Archaeology, Cairo University 1997. Gained M.Sc. in metals conservation from conservation department, faculty of Archaeology, Cairo University 2006. Gained Ph.D. in metals conservation from conservation department, Archaeology faculty, Sohag University 2013. Physicist in the scientific laboratories in the Conservation researches center, Supreme Council of Antiquities, Egypt from 1998. General supervisor of Scientific Labs, Grand Egyptian Museum, Ministry of Antiquities 2010. PHD holder researcher at Post Graduate Studies College of Nanotechnology, Cairo University; and Head of Computerized Tomography X-ray unit, Cairo Egyptian Museum, Ministry of Antiquities, Egypt.

Yussri Salem Mahrous Ali
yousry.ali@arch.svu.edu.eg
Conservation Department, Faculty of Archaeology, South Valley University, Qena, Egypt.

BSc., BA, PhD in Study and conservation of archaeological metals and their alloys. lecturer in conservation department at faculty of archaeology at south valley University. He is research interests include: Study and conservation of archaeological metals and their alloys, corrosion and corrosion inhibition of archaeological metals, electrochemical techniques in metal conservation, innovative analytical techniques applied to conservation science, and archaeometallurgy. Lecturer at the Department of Restoration, South Valley University.

Artículo enviado el 25/01/2021
Artículo aceptado el 01/06/2021

https://doi.org/10.37558/gec.v19i1.898